Numerical Simulation of Orographic-Convective Rainfall with Kuo and Betts-Miller Cumulus Parameterization Schemes

By Kiran Alapaty, Rangarao V. Madala[1] and Sethu Raman

Department of Marine, Earth and Atmospheric Sciences, North Carolina State University, Raleigh, N.C. 27695-8208, U.S.A.

(Manuscript received 22 March 1993, in revised form 13 December 1993)

Abstract

Two different cumulus parameterization schemes, one developed by Kuo and the other by Betts-Miller, are used to simulate the orographic-convective rainfall associated with the Western Ghats for two days during which monsoon rainfall was moderate to heavy. A ten-layer primitive equation limited area nested grid model is used to perform numerical simulations. It is found that predicted rainfall near the Western Ghats with the Kuo scheme agrees well with the observations. With the Betts-Miller scheme, model failed to predict rainfall over this region.

To find out uncertainties in the adjustment parameters used in the Betts-Miller scheme, five sensitivity experiments are performed. Different values are assigned to the two adjustment parameters, namely the relaxation time scale and the saturation pressure departure, in each of the sensitivity experiments. Results from these sensitivity studies indicate that specification of relaxation time scale depends on the model horizontal resolution. Relaxation time scale needs to be smaller as the model horizontal resolution increases. Also, rainfall predictions are less sensitive to different values of relaxation time scales than those for the saturation pressure departure. Variations in the prescribed thermodynamic reference profiles caused by small prescribed changes in the values of saturation pressure departure led to improvements in the rainfall predictions. It was also found that there exists a lower limit on the values of relaxation time scales and saturation pressure departures for the monsoon region beyond which predicted rainfall rates do not show further improvement.

1. Introduction

Cumulus convection is an important physical process that influences the dynamic and thermodynamic state of the tropical atmosphere. It is included in numerical models either explicitly or in parameterized form depending on the model horizontal grid resolution. Since convective elements have a horizontal length scale of the order of 0.1 – 10 km, fine horizontal resolution is required in numerical models for an explicit treatment of the convective processes. On the other hand, parameterization schemes allow us to use coarser grid resolution in numerical simulations. Except the hybrid-closure schemes, cumulus parameterization schemes can be categorized into three groups: the moisture convergence scheme (Kuo, 1965, 1974), the mass-flux type scheme (Arakawa and Schubert, 1974), and the moist convective adjustment scheme (Manabe *et al.*, 1965).

Because of its simplicity and ease of implementation in numerical models compared to mass-flux type schemes, the Kuo scheme is widely used in several research and operational models. The original Kuo (1965) scheme had a tendency for too much moistening of the atmosphere. A moistening parameter (b) was introduced to correct this tendency (Kuo, 1974). Since a proper choice of b is crucial for estimating convective heating and moistening rates, several studies (*e.g.*, Anthes, 1977; Geleyn, 1985) have been made to estimate this parameter. A semiprognostic study using several versions of the Kuo scheme for the Indian summer monsoon period was done by Das *et al.* (1988). Their results showed that the 1974 Kuo scheme provides considerable improvement in simulating the heating, moistening, and rainfall rates when combined with the moistening parameter proposed by Anthes (1977). They also noticed that the choice of small (almost equal to zero) moistening parameter can cause unrealistic drying of the atmosphere.

Based on observational studies Betts (1982, 1986) proposed a new convective adjustment scheme which includes both deep and shallow convection. The

[1]Present affiliation: Naval Research Laboratory Washington, D.C. 20375, U.S.A.

deep convection scheme is similar to the other moist convective adjustment schemes except that it uses observed quasi-equilibrium thermodynamic profile as a reference state rather than a moist adiabat. Baik *et al.* (1990a and b) incorporated the Betts-Miller scheme in an axisymmetric tropical cyclone model and showed that the scheme can simulate developing, rapidly intensifying, and mature stages of a tropical cyclone starting from a weak initial vortex. Their results indicated that simulated idealized tropical cyclone is sensitive to the saturation pressure departure, an adjustment parameter in the Betts-Miller scheme. In the present study, we will use a version of the Betts-Miller scheme similar to that used by Baik *et al.* (1990a).

Junker and Hoke (1990) compared performances of the 1965 Kuo scheme and the Betts-Miller scheme in predicting rainfall during winter season over the southern United States with the NMC (National Meteorological Center) nested grid model. The Betts-Miller scheme gave favorable precipitation scores, but it showed the tendency for the mid-latitude cyclones to overdeepen. Puri and Miller (1990) studied the sensitivity of the cumulus parameterization schemes to the structure of four tropical cyclones observed during the AMEX (Australian Monsoon Experiment). Their results showed better vertical consistency when the Betts-Miller scheme is used in comparison to the Kuo scheme. Bothe the analyses and forecasts showed considerable sensitivity to the Betts-Miller scheme by generating more intense cyclonic systems as compared to the Kuo scheme. Their result is somewhat consistent with that of Junker and Hoke (1990). The Betts-Miller scheme has been used in the past either to simulate observed tropical or mid-latitude cyclones with a coarse horizontal resolution (>80 km). It will be of interest to study the performance of the Betts-Miller scheme in simulating the orographic-convective precipitation in a model with a finer resolution. Simulation of the orographic-convective precipitation associated with the Western Ghats, a mountain range of about 1 km high along the west coast of the Indian peninsula, will be the subject of this paper.

During the southwest monsoon season (June to September), west coast of India is one of the areas where heavy rainfall rates are observed very frequently. This region is of particular interest because (i) lower level westerlies approach the Western Ghats almost at right angles after traveling thousands of kilometers over the warm Indian Ocean and the Arabian Sea, and (ii) convective instability, which can trigger deep convection giving rise to convective rainfall, exists. These mountains running parallel to the west coast are located about 50 km inland. Figure 1 shows the domain of simulation in the Coarse-Grid Mesh (CGM) and the Fine-Grid Mesh (FGM), the latter being located over India and the surrounding oceans.

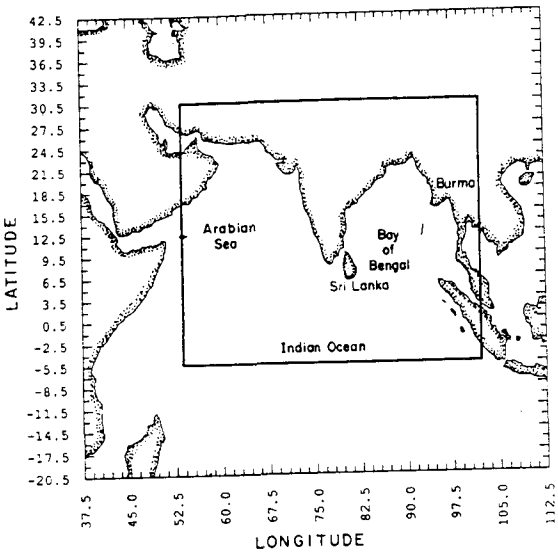

Fig. 1. The model domain of numerical simulation in the Coarse-Grid Mesh (CGM) and the Fine-Grid Mesh (FGM).

An analytical study of Smith and Lin (1983) using a steady-state linear model concluded that in the absence of convective instability the dynamic forcing by the Western Ghats is insufficient to produce the observed rainfall rates. Utilizing the aircraft observations over the Arabian Sea and using a nonlinear mountain-flow interaction model, Grossman and Durran (1984) concluded that the Western Ghats are responsible for offshore convection. The lifting predicted by a model was applied to mean dropwindsonde soundings for the days with and without offshore convection and it was found that spells in the rainfall can be attributed to the cooler surface layer and the dry layer above the boundary layer which might have originated from the Arabian desert. In a numerical study using the PSU/NCAR mesoscale model Vukicevic and Errico (1990) found that topography has an important role in the predictability of the mesoscale and synoptic-scale circulations. So, it is important to represent mountains realistically in three dimensional numerical simulation studies to capture their important role. Using a cloud model, Ogura and Yoshizaki (1988) showed that the fluxes of sensible heat and moisture from the ocean and vertical wind shear are two important factors that decide the intensity and location of the rainfall near the Western Ghats. An observational study of cloud diameter and height ratios by LeMone (1989) also shows that vertical shear of the horizontal wind may enhance convective precipitation. This is in agreement with a numerical study of Ogura and Yoshizaki (1988) indicating the importance of wind shear in

the vertical near the Western Ghats.

The above studies of orographic-convective rainfall are two dimensional and have some limitations. Smith and Lin (1983) specified the heating over the ocean and Grossman and Durran (1984) omitted air-sea interactions, latent heating and wind shear. Even though these studies gave some insight into the physical processes involved, they cannot simulate the observed spatial and temporal variation of rainfall. In order to simulate the observed rainfall rates more realistically, one needs a nonlinear three dimensional model. Such a model should have proper representation of dynamics, thermodynamics, topography and relevant physics.

Significant features of the problem of orographic-convective rainfall near the Western Ghats can be summarized as follows:

i) The Western Ghats cause the orographic lifting of the air parcels.

ii) Convective instability over this region can lead to deep convection.

iii) Moisture flux from the Arabian Sea can contribute to the rainfall.

iv) Vertical wind shear can alter the location and the amount of the rainfall.

These processes should be realistically represented to simulate the observed spatial and temporal structure of the orographic-convective rainfall. In addition, the model domain must be sufficiently large to simulate the synoptic-scale circulations.

The paper compares the simulated orographic-convective rainfall near the Western Ghats region using a three dimensional limited area nested grid model with the Kuo and the Betts-Miller cumulus parameterization schemes.

2. The model

2.1 *Governing equations*

The present study utilizes a nested grid model developed at the Naval Research Laboratory and North Carolina State University based on the limited area dynamical weather prediction model developed earlier by Madala *et al.* (1987). It is primitive equation model written in pressure-based σ-coordinate system having a one-way interacting nested grid network. The σ-coordinate is defined by $\sigma = p/p_s$, where p is the pressure and p_s the surface pressure. Various physical processes are include in the model either explicitly or in parameterized form and are discussed below.

2.2 *Physical processes*

The model physics includes latent heat, sensible heat, and momentum exchange between the boundary layer and the underlying surface using the surface layer similarity theory (Businger *et al.*, 1971), grid-scale precipitation, dry convection, and diffusion processes. Moist convective parameterization schemes used in the model are described in the next subsection. The short and long wave radiative processes are not included in the present model. A second-order diffusion for momentum on σ-surfaces and for heat and water vapor on p-surfaces is used to account for the cascading of energy into unresolved subgrid-scale waves. If super-saturation exists at any level, the excess moisture is assumed to condense and fall out to the next lower layer and evaporate or continue to fall depending upon the degree of the saturation at that level. The model has a dry convective adjustment procedure to remove dry convective instability that can occur during model integration.

2.2.1 *Kuo cumulus parameterization scheme*

Kuo's (1965) parameterization scheme accounts for the effects of cumulus convection and resulting changes in the large-scale humidity and temperature fields. The heating (Q_T) and moistening (Q_q) imparted to the environment by the cumulus clouds is assumed to be proportional to the temperature and specific humidity differences between the environment and the cloud and can be written as (Kuo, 1974)

$$Q_T = \frac{gL(1-b)M_t\,(T_c - T_g)}{c_p\,(p_a - p_t)\,\langle T_c - T_g\rangle}, \tag{1}$$

$$Q_q = \frac{gbM_t\,(q_c - q_g)}{(p_a - p_t)\,\langle q_c - q_g\rangle}, \tag{2}$$

respectively, where g is the gravitational acceleration, L the latent heat of evaporation, M_t the total moisture accession rate per unit horizontal area, and p_a and p_t the pressures at the lowest model level and at cloud top, respectively. The quantities in the angular bracket represent the values averaged from $p = p_t$ to p_a. The subscripts g and c stand for model grid-point value and cloud, respectively. T_c and q_c are the temperature and specific humidity on the moist adiabat passing through the lifting condensation level of an air parcel at the lowest model level. The moistening parameter b is calculated according to the method suggested by Anthes (1977) and is given by

$$b = [1 - \langle RH_g\rangle]^n, \tag{3}$$

where $<RH_g>$ is the mean environmental relative humidity averaged from $p = p_t$ to $p = p_a$. We have used $n = 3$ for the moisture partitioning in the Eq. (3) consistent with the study on the convective heating rates over the monsoon region (Das *et al.*, 1988).

2.2.2 Betts-Miller deep cumulus parameterization scheme

The Betts-Miller convective adjustment scheme assumes that in the presence of cumulus convection, the local thermodynamic structures are constrained by the convection and adjusted towards observed quasi-equilibrium thermodynamic state. The convective heating (Q_T) and moistening (Q_q) terms are represented by

$$Q_T = \frac{T_r - T_g}{\tau}, \tag{4}$$

$$Q_q = \frac{q_r - q_g}{\tau}, \tag{5}$$

where the subscript r denotes the reference state and g the grid-point value before convection and the factor τ is the adjustment (or relaxation) time scale. The adjustment time scale represents the lag between the large-scale forcing and the convective response. The Betts-Miller scheme contains shallow convection as well as deep convection. However, since the Kuo scheme deals with the deep convection, only the deep convection part of the Betts-Miller scheme is used for the comparative purpose. The stability weight on the moist adiabat is a measure of instability and determines the slope of the reference profile with respect to the moist adiabat. The saturation pressure departure is a measure of subsaturation, *i.e.*, how far an air parcel must be vertically displaced to become saturated and hence is a measure of relative humidity. The stability weight on the moist adiabat, relaxation time scale and the saturation pressure departure at the lowest model level are specified as 0.8, 7200 sec and −30 hPa, respectively.

2.3 Numerical method and nesting technique

The time integration scheme utilized in the present model is a split-explicit method which allows a larger time step by effectively separating various terms in the prognostic equations into parts governing slow-moving Rossby modes and fast-moving gravity modes. For the first and second fast-moving gravity modes smaller time step is used and for all other modes a larger time step is used. The implementation of these varying time steps is the basis for the split-explicit method. The time steps for the slow moving modes in the CGM and the FGM are 300 s and 100 s, respectively, and appropriate smaller time steps satisfying CFL criterion are used for the fast-moving modes. For further details, reader is referred to Madala *et al.* (1987). For the horizontal differencing, a staggered grid network (Arakawa C-grid) is used with p_s, q, T, ϕ, $\dot{\sigma}$, specified at the same horizontal points, and u and v interlaced between them where p_s is the surface pressure, q the specific humidity, T the temperature, ϕ the geopotential, $\dot{\sigma}$ the vertical velocity of σ, u the zonal wind velocity, and v the meridional wind velocity, respectively. The finite difference technique used in the model is second-order accurate. It conserves total energy, mass, and momentum in the absence of the heat and momentum sources.

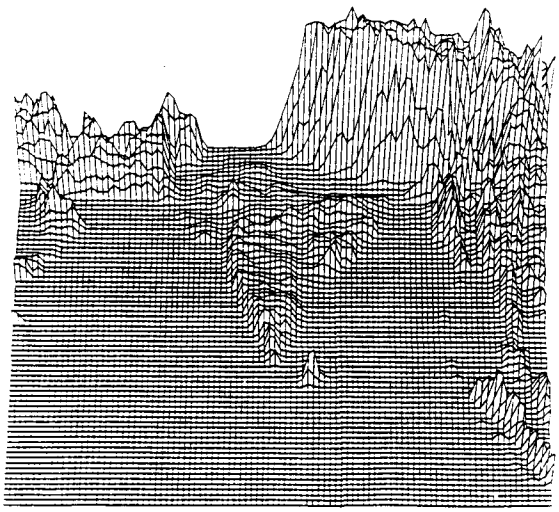

Fig. 2. The topography in the Fine-Grid Mesh (FGM). Large surface elevations over the northern region are the Himalayan mountains and the Western Ghats are located along the west coast of India.

In the present version of the model, the FGM overlaps one-third of the CGM and the FGM is nested into the CGM such that every third grid point in the FGM is collocated with that in the CGM. The nested grid is positioned so that its boundary rows and columns overlap the CGM interior rows and columns. This nesting configuration enables the Fine-Grid Mesh domain boundary values to be specified by the Coarse-Grid Mesh interior grid points.

2.4 Model domain, topography and sea surface temperature

Analyzed data from the European Centre for Medium-Range Weather Forecast (ECMWF) are utilized to specify the initial conditions. Analyzed data are of 1.875° resolution at 14 vertical levels. Bicubic polynomial interpolation technique is used for the horizontal interpolation to model grid points. Horizontal grid resolutions in the CGM and the FGM domains are 1.5° and 0.5°, respectively, and the vertical grid resolution in σ-coordinate is 0.1. The CGM domain covers from 37.5°E to 112.5°E and 20.5°S to 42.5°N and the FGM domain from 54°E to 102°E and 5.5°S to 30.5°N (Fig. 1).

Model topography was obtained from the navy 10′ global topography data for 1.5° and 0.5° horizontal resolutions. Figure 2 shows the fine grid topog-

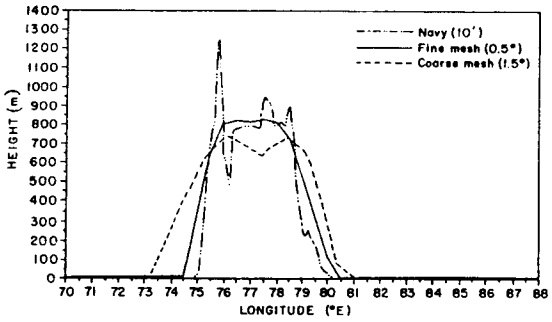

Fig. 3. The cross section of the Western Ghats at 13°N in the CGM and the FGM along with the navy 10′ data.

raphy. Large surface elevations over the northern region are the Himalayan mountains. The Western Gahats are located along the west coast of India. The Western Ghats extend about 1600 km in a north-south direction with average heights of 800–900 m although individual peaks have heights exceeding 1200 m. Orographic lifting of the humid monsoon westerlies causes heavy rainfall over this region. The cross sections of the topography at 13°N in the CGM and the FGM along with the actual 10′ data are shown in Fig. 3. Comparison of surface elevation data in the CGM and in the FGM domains shows that the mountains are higher and steeper in the FGM domain than in the CGM domain. Peak of the Western Ghats is ~725 m in the CGM domain and ~850 m in the FGM. Peaks are at different locations for different model grid resolutions. The ten minute topography data (Fig. 3) indicates that the Western Ghats peaks are about 100 km away from the west coast. In the coarse-grid domain peaks are located one grid point (~150 km) from the coast and in the fine-grid domain these are located two grid points (~100 km) away from the coast. Model sea surface temperatures (SST) were obtained from the 1° resolution global climatological values based on a 10 year average for the month of July.

2.5 Boundary conditions

Davies scheme (1976, 1983) is employed to provide lateral boundary conditions in the present version of the model. For any independent variable a, it can be written as

$$a = (1 - \alpha)a_m + \alpha a_b, \tag{6}$$

where the subscript m represents model-computed values and the subscript b represents the boundary values obtained either from observations or from coarser version of the model. The merging is done over six grid points at the boundaries of both domains. The α is defined as a quadratic function of the minimum distance from the lateral boundary in units of the grid spacing (Gronas *et al.*, 1987). At each time step, the boundary values a_b for the coarse grid are obtained through a linear interpolation in time from the ECMWF analysis at 24 hour intervals. For the FGM domain, lateral boundary conditions a_b are obtained through a linear interpolation in time and space from the CGM domain. Also, for consistency, topographic heights at the lateral boundaries of the FGM are specified same as those in the CGM domain. At the model top and bottom, the boundary condition for $\dot{\sigma}$ is zero.

2.6 Numerical experiments

Numerical simulations are performed for 48 hours starting at 12 UTC 12 July 1988 using either the Kuo or the Betts-Miller cumulus parameterization scheme. Coastline in both the CGM and the FGM domains are determined by the model topography data. Darker lines in all horizontal space plots, *e.g.*, Figs. 5, 6, etc..., represent the model coastline.

3. Synoptic conditions

During the simulation period, from 12 UTC 12 July to 12 UTC 14 July 1988, monsoon was moderately active over the Indian subcontinent. Figure 4a and 4b show the cumulative rainfall ending at 03 UTC 13 and 14 July 1988, respectively. Due to the orographic lifting and associated convection, heavy rain occurs along the west coast of India. Seaward increase of rainfall indicates that the maximum rainfall associated with the Western Ghats during this period seems to be located offshore. Maximum rainfall just offshore of the west coast of India is about 100 and 140 mm d^{-1}, respectively for the two days. Rainfall was also observed over the central regions of India with a maximum of about 100 to 140 mm d^{-1} during the period of simulation.

4. Discussion of results

Results from the numerical simulations are compared with the observations in this section. In the following, model results with the Kuo and the Betts-Miller schemes are referred to as the KUO and the BMS, respectively.

Predicted rainfall (mm d^{-1}) for the first day of simulation for the CGM domain in the KUO and the BMS are shown in Fig. 5a and 5b, respectively. Rainfall predictions are quite different with the KUO and the BMS. Predicted rainfall along the west coast of India with the KUO is about 20 mm d^{-1} while the BMS predicts no rainfall. Observations indicate rainfall about 100 mm d^{-1} along the west coast. Both the schemes predict a rainfall of about 20 mm d^{-1} over central regions of India, but again much lower than the observations. Model-predicted rainfall for the first day of simulation for the FGM domain in the KUO and the BMS are shown in Fig. 5c and 5d, respectively. Finer horizontal resolution

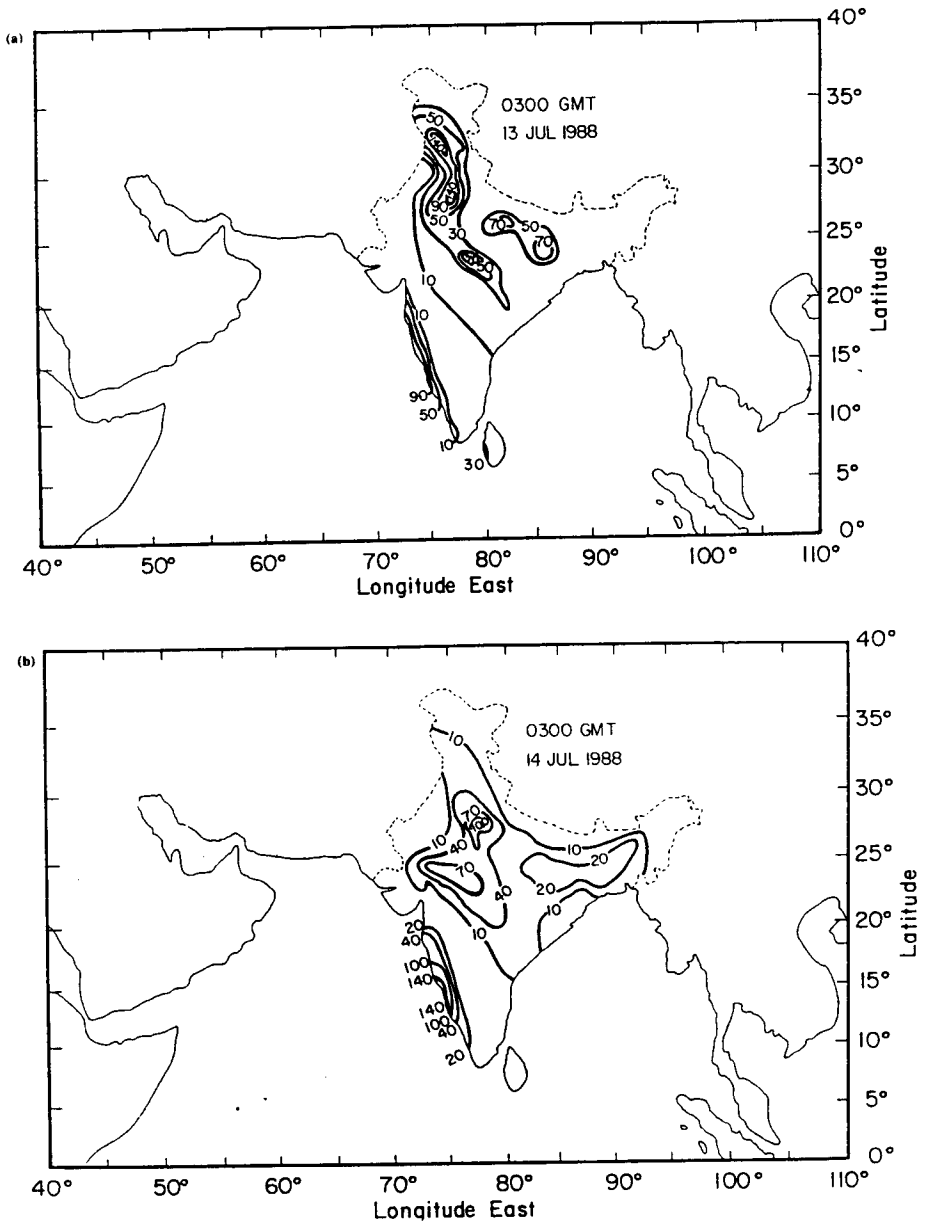

Fig. 4. Accumulated rainfall distribution ending at (a) 03 UTC 13 and (b) 03 UTC 14 July 1988.

in the FGM resulted in higher rainfall rates in both the schemes. In the KUO, predicted rainfall along the west coast of India is closer to the observations with a maximum of about 73 mm d^{-1} located offshore. With the Betts-Miller scheme model again fails to predict rainfall along the west coast except about 10 mm d^{-1} over a small region offshore (over the Arabian Sea). Over land, rainfall rates predicted by the KUO and the BMS are lower than those in the observations. However, with the Kuo scheme predicted rainfall values are somewhat closer to the observations than those with the Betts-Miller scheme.

Predicted rainfall for the CGM domain for the second day of simulation in the KUO and the BMS are shown in Fig. 6a and 6b, respectively. About 140 mm d^{-1} of rainfall was observed offshore of the west coast of India (Fig. 4b). The spatial distribution of observed rainfall is somewhat similar to the previous day (July 13) but with relatively higher rates along the west coast of India. In the KUO, the model predicts a rainfall maximum of about 48

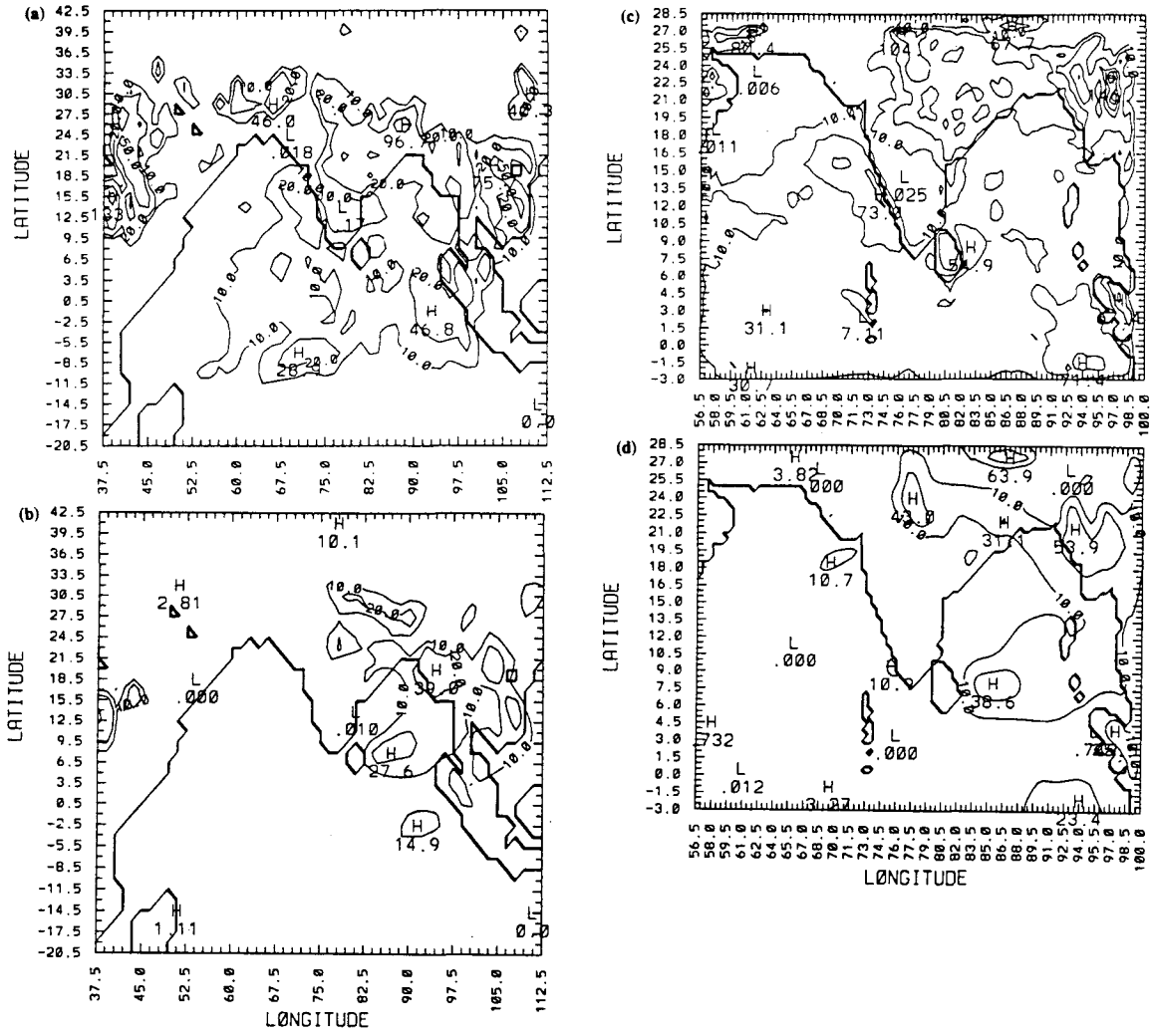

Fig. 5. Predicted rainfall for the CGM domain for a period of 24 hours ending at 12 UTC 13 July 1988 in the (a) KUO and the (b) BMS, respectively. Contour intervals are 10, 20, 50, 80 mm d^{-1}. Predicted rainfall for the FGM domain for a period of 24 hours ending at 12 UTC 13 July 1988 in the (c) KUO and the (d) BMS, respectively. Contour intervals are 10, 25, 50, 75, 100 mm d^{-1}.

mm d^{-1} offshore of the west coast of India, about one-third of the observed value. In the BMS, model predicts a rainfall maximum of about 13 mm d^{-1} over the same region, but for a smaller area. In general, over land, predicted rainfall rates with the Kuo scheme are closer to the observations than with the Betts-Miller scheme. Figure 6c and 6d show predicted rainfall for the FGM domain for the second day of simulation in the KUO and the BMS, respectively. In the KUO, predicted rainfall maximum is just offshore of the west coast of India with a maximum of about 144 mm d^{-1}, very similar to the observed value. In the BMS, model predicts rainfall maximum just offshore of the west coast of India with a maximum of about 23 mm d^{-1}, In the BMS, model predicts very little rainfall over the Arabian Sea (less than 0.1 mm d^{-1}) while the KUO predicts larger rainfall rates. It is difficult to compare the relative performances of the Kuo and the Betts-Miller schemes in data sparse regions such as the oceans. However, over the central regions of India, the KUO predicts rainfall somewhat closer to the observations while the BMS predicts lower rates.

In summary, predicted spatial distributions of rainfall offshore of the west coast of India with the Kuo scheme are in good agreement with the observations for the two days of simulation for the FGM. As expected, predicted rainfall rates are larger for the fine-grid domain as compared to the coarse-grid

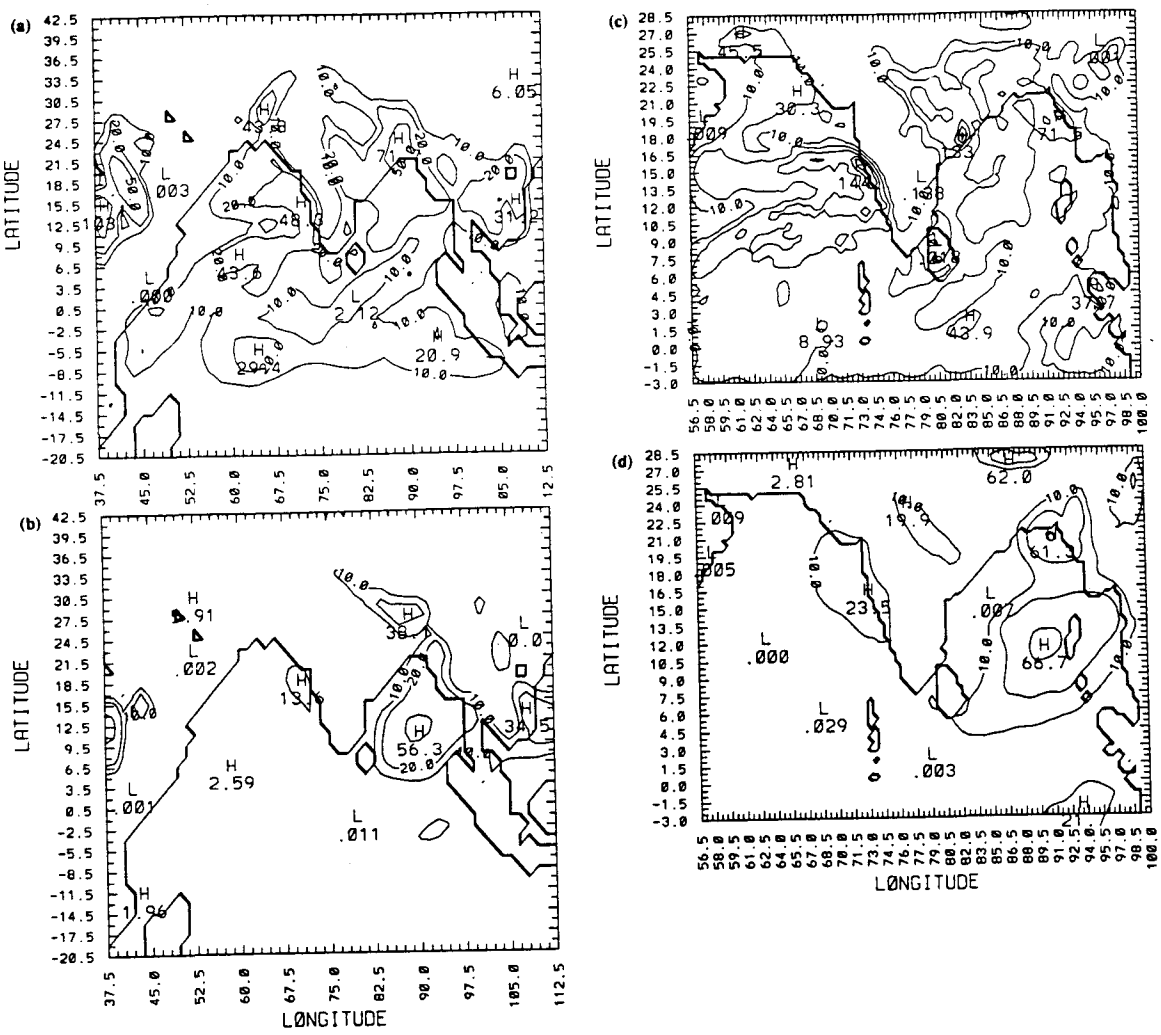

Fig. 6. Predicted rainfall for the CGM domain for a period of 24 hours ending at 12 UTC 14 July 1988 in the (a) KUO and the (b) BMS, respectively. Contour intervals are 10, 20, 50, 80 mm d^{-1}. Predicted rainfall for the FGM domain for a period of 24 hours ending at 12 UTC 14 July 1988 in the (c) KUO and the (d) BMS, respectively. Contour intervals are 10, 25, 50, 75, 100, 125, 150 mm d^{-1}.

domain for the cumulus parameterizations. Model fails to predict the observed spatial and temporal distribution of rainfall when the Betts-Miller scheme is used. Convective adjustment parameters in the Betts-Miller scheme used in this study are good only for tropical cyclone simulations (Betts, 1986; Baik *et al.*, 1990; Puri and Miller, 1990). For the monsoon region, particularly for the orographically induced rainfall, validity of these parameters need to be studied. Flow patterns and associated thermodynamic structure of the atmosphere for a tropical cyclone are different from those present in the monsoon circulations. Also, unlike in a tropical cyclone monsoon westerlies are humid only up to about 400 hPa. Analyzed data indicate presence of strong vertical shear from surface to tropopause near the Western Ghats region and cumulus convection can be influenced by this shear present in the environment. For these reasons, several sensitivity studies are performed with the Betts-Millers scheme.

Sensitivity studies on the simulation of an idealized axisymmetric tropical cyclone (Baik *et al.*, 1990) with the Betts-Miller scheme indicated that their model predictions are very sensitive to two convective adjustment parameters, namely, relaxation time scale and saturation pressure departure. Other convective adjustment parameters in the Betts-Miller scheme such as stability weight on moist adiabat, etc..., were found to have lesser significance on their model predictions. In view of the model failure to predict observed rates of rainfall with the Betts-Miller scheme in the present study,

Table 1. List of sensitivity experiments with the Betts-Miller Scheme

CASE	τ (s)	S (hPa)	Grid
CASE-1	7200	−30	CGM & FGM
CASE-2	3600	−30	CGM & FGM
CASE-3	3600	−30	CGM
	1200		FGM
CASE-4	1800	−30	CGM
	600		FGM
CASE-5	1800	−40	CGM
	600		FGM
CASE-6	1800	−50	CGM
	600		FGM

sensitivities of rainfall predictions to the two convective adjustment parameters (relaxation time scale and saturation pressure departure) with the Betts-Miller scheme are studied in the following section.

4.2 Sensitivity of rainfall predictions to convective adjustment parameters

Five sensitivity experiments are performed by assigning different values for relaxation time scale (τ) and saturation pressure departure (S) parameters. Table 1 shows the values assigned for the τ and the S in each of the sensitivity experiment. As mentioned earlier, the coarse-grid domain is referred to as the CGM and the fine-grid to as the FGM. Simulation results with the Betts-Miller scheme described above are considered as those for the control experiment and is referred to as CASE-1 in the Table 1. In the simulations from CASE-1 to CASE-4 saturation pressure departure is kept the same while the relaxation time scale is decreased from 7200 to 600 s. Note that relaxation time scales are different for the CGM and the FGM from CASE-3 through CASE-6. Betts (1986) found that for a given S value there was a limit for τ in the model used at ECMWF and it also strongly depended on the model horizontal resolution. For this reason we also selected different relaxation time scales for the CGM and the FGM.

The adjustment or relaxation time scale parameter (τ) determines the lag of the convective response to large-scale forcing. As the τ values becomes smaller, adjustment of the model atmosphere towards specified thermodynamic reference profile will become more rapid. On the other hand, usage of larger τ values will result in increased grid scale rainfall. For Indian monsoon region, observations indicate that most of the rainfall is from the deep cumulus convection while large scale rainfall is smaller. So, for the monsoon region relaxation time scale should be smaller and should be on the order of two hours or less. The saturation pressure departure (S) is related to the subsaturation and hence to the equilibrium relative humidity. Though it does not significantly influence the equivalent potential temperature but a decrease in S value will lead to warming and drying of the vertical column in the model. In other words, decrease in S should lead to an increase in sub-grid scale rainfall.

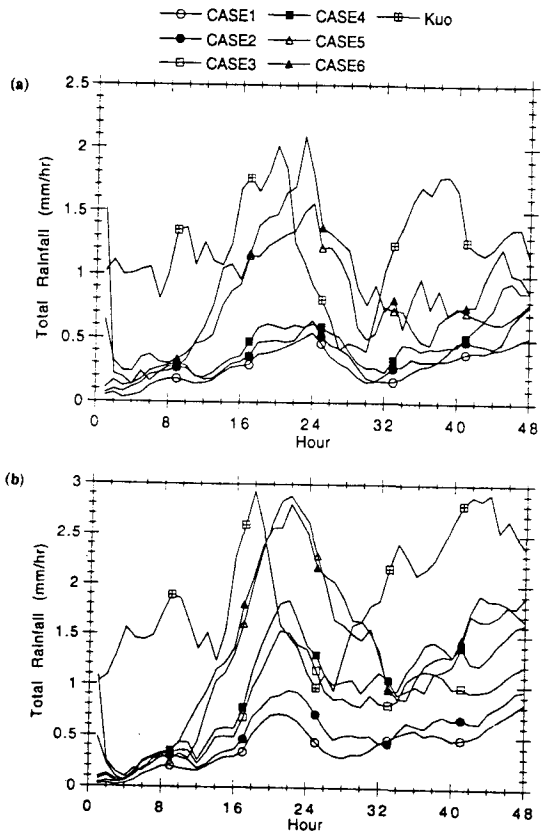

Fig. 7. Temporal variation of the averaged total rainfall for the area 8° to 20°N and 70.5° to 76.5°E for the (a) coarse-grid domain and (b) fine-grid domain in all numerical experiments.

In order to compare the effects of different values of relaxation time scale and saturation pressure departure on the model predictions, area-average of predicted rainfall over an area, 8° to 20°N and 70.5° to 76.5°E covering most of the region surrounding the Western Ghats is considered. Figure 7a and 7b show temporal variation of area-averaged total rainfall for the above region for the CGM and the FGM domains, respectively. Decrease of the relaxation time scale, τ, from 7200 to 1800 s, *i.e.*, from the CASE-1 through CASE-4 had little effect on the predicted total rainfall. In general, there is a slight increase in rainfall rates from the starting time to end of the simulation period (Fig. 7a) for the CGM domain. When the saturation pressure departure, S, is decreased from −30 to −50 hPa there exists major differences in the predicted rainfall rates, particularly after ninth hour of simulation. Also, during

the first two hours of simulation a decrease in the S resulted in large rainfall rates and is indicated by a spike in the CASE-5 and CASE-6. This is due to the fact that decrease in the S value caused reference profiles for temperature and specific humidity to deviate largely from the model soundings over these convectively active regions resulting in large rainfall rates. This indicates some uncertainty in the initial conditions. After the adjustment period of two hours, predicted rainfall rates are similar to those in the other cases. For the monsoon region, variations in the S have larger impact on the model predictions than variations in the τ. Also, rainfall rates in the CASE-6 are almost higher than those in the rest of the simulations.

On the other hand, rainfall predictions for the FGM domain (Fig. 7b) show some differences as compared to those in the CGM domain. Decrease of τ from CASE-1 through CASE-4 indicate continuous increase in the predicted rainfall rates. Decrease in the S values resulted in further increased rainfall rates. Also, differences in the predicted rainfall rates between the CASE-5 and the CASE-6 on average and very small (less than $0.1\,\mathrm{mm\,hr^{-1}}$) as compared to those in the CGM domain. This result indicates that further decrease in the S and the τ values for the FGM domain may not result in significant increase in the predicted rainfall rates. But, for the CGM domain, further decrease in these adjustment parameters may give slightly increased rainfall rates. Rainfall rates predicted in the CASE-6 for the CGM and the CGM domains on average are higher than those in the rest of the cases. It can be seen that for both the CGM and the FGM domains, rainfall predictions are more sensitive to the values of S than to the values of τ. Predicted rainfall rates with the Kuo scheme show earlier occurrence of rainfall maxima during the first day of simulation while the rainfall maximum with the Betts-Miller scheme lags behind by about four hours. After 30 hours of simulation, rainfall rates predicted with the Kuo scheme are much higher than those with any of the simulations using the Betts-Miller scheme.

Temporal variations of area-averaged evaporation for the region between 8° to 20°N and 70.5° to 76.5°E for the CGM and the FGM domains are shown in Fig. 8a and 8b, respectively. Temporal average of the predicted evaporation rate with the Kuo scheme is about $0.16\,\mathrm{mm\,hr^{-1}}$ for the CGM while with the Betts-Miller scheme (in all cases) it is relatively higher. This is due to the fact that the Kuo scheme dried upper layers of the atmosphere more than those near cloud base. This resulted in humid layers near to the surface limiting the evaporation rates. On the other hand, results obtained using the Betts-Miller scheme indicated weaker vertical gradients in the convective heating profiles with relatively drier layers near to the surface as compared to those

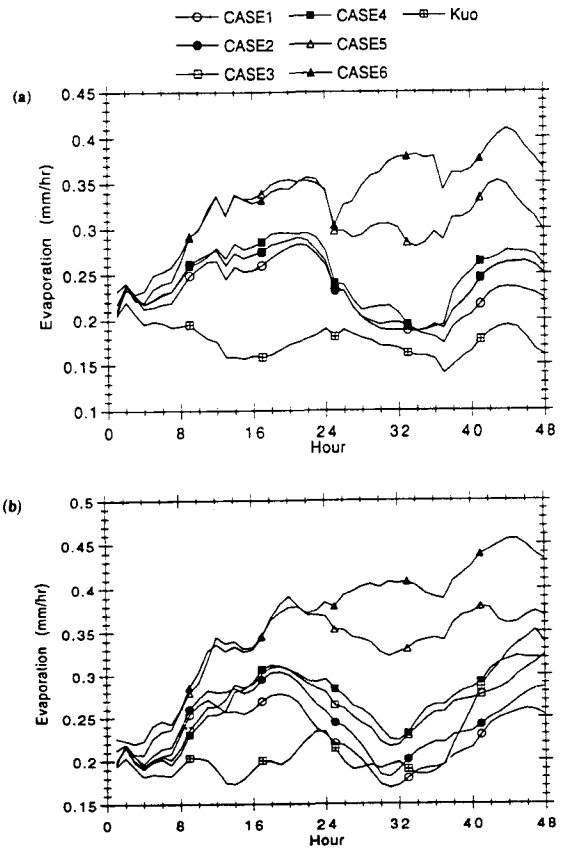

Fig. 8. Temporal variation of the averaged evaporation for the area 8° to 20° and 70.5° to 76.5°E for the (a) coarse-grid domain and (b) fine-grid domain in all numerical experiments.

present in the KUO. This factor along with the differences in the wind speeds led to larger evaporation rates in the BMS. For the FGM (Fig. 8b) evaporation rates are somewhat similar to those in the CGM but are slightly higher. Also, after 24 h of simulation average evaporation rates in the KUO as well as in the CASE-1 through CASE-4 are somewhat similar for the FGM. Circulation patterns associated with the deep cumulus convection are only marginally different for CASE-1 through CASE-4. Interestingly, decrease in saturation pressure departure values in CASE-5 and CASE-6 caused increased evaporation rates in the CGM and FGM. This is due to the fact that decrease in the S values triggered intense cumulus convection. Increased convective heating caused stronger circulation patterns over this region leading to stronger surface-level winds, which resulted in increased evaporation.

In order to analyze the effects of different values of the S and τ on the grid scale and sub-grid scale rainfall, area-averages for the region between 8° to

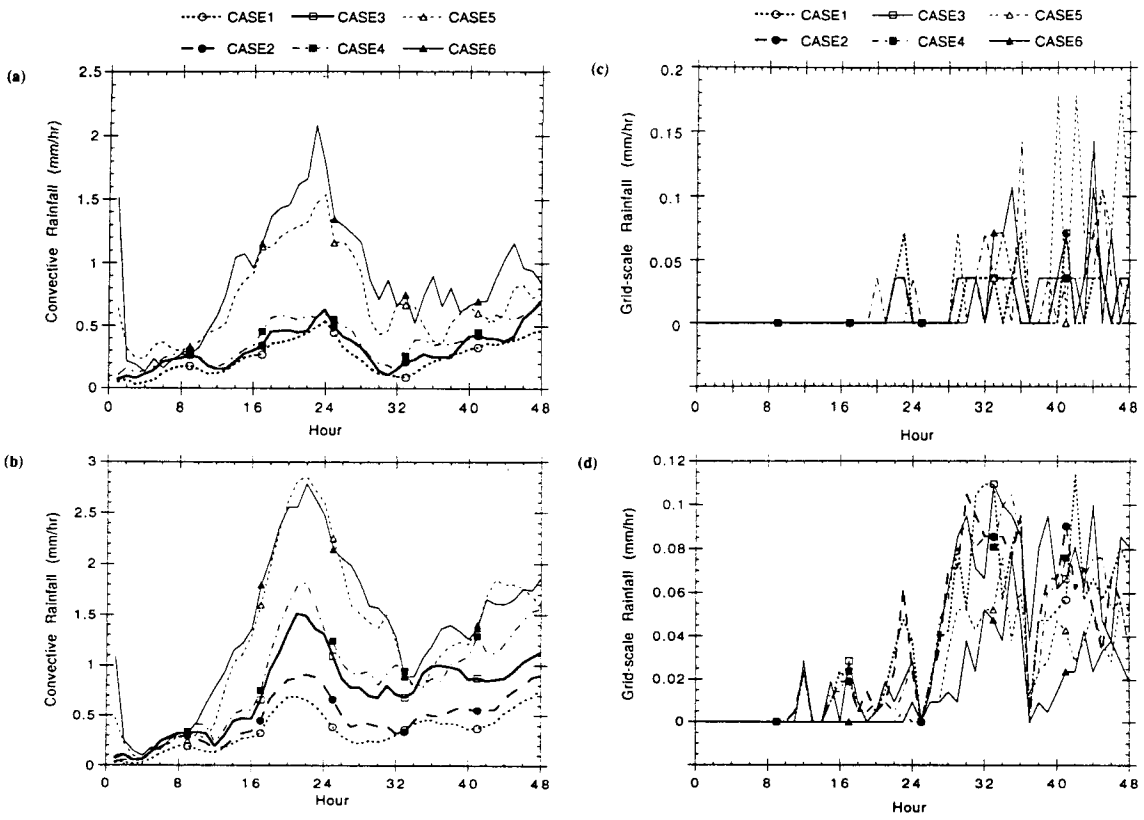

Fig. 9. Temporal variation of the averaged sub-grid scale rainfall for the area 8° to 20°N and 70.5° to 76.5°E for the (a) coarse-grid domain and (b) fine-grid domain in all numerical experiments. Temporal variation of the averaged grid-scale rainfall for the area 8° to 20°N and 70.5° to 76.5°E for the (c) coarse-grid domain and (d) fine-grid domain in all numerical experiments.

20°N and 70.5° to 76.5°E is considered. Figure 9a and 9b show temporal variation of area-averaged sub-grid scale (parameterized) rainfall for the CGM and the FGM, respectively for all the cases (CASE-1 through CASE-6) using the Betts-Miller scheme. Note that sub-grid scale rainfall rates are very similar to the total rainfall rates (shown in Fig. 7a and 7b). This is expected because most of the rainfall over the monsoon region is from the deep cumulus convection. Temporal variation of area-averaged grid scale rainfall for the CGM and the FGM are shown in Fig. 9c and 9d, respectively. It can be seen that grid scale rainfall rates are about an order of magnitude smaller than the sub-grid scale rainfall rates for the CGM and the FGM domains. Consistently, increased horizontal resolution in the FGM domain resulted in reduced grid scale rainfall rates as compared to those rates in the CGM domain. For the CGM and the FGM domains there is a continuous decrease in grid scale rainfall from CASE-1 to CASE-4. In the CASE-5 the S value is lower than that in the CASE-1, CASE-2, CASE-3 and CASE-4. Decreased S value in CASE-5 leads to increased grid scale rainfall, as a result of stronger vertical circulations, as explained earlier. But further decrease in the S value in CASE-6 also results in further decrease in the grid scale rainfall.

The construction of reference profiles and the specification of the relaxation time scales are the two major components of the Betts-Miller cumulus parameterization scheme. It can be seen from the above discussed results that model predictions of rainfall depend more strongly on the saturation pressure departure parameter rather than on the relaxiation time scale. Also, constructed reference profiles for moisture are based on the saturation pressure departure parameter and hence rainfall predictions are more sensitive to the S values. These results are consistent with the sensitivity experiments with an axisymmetric tropical cyclone model (Baik *et al.*, 1990b). Their results indicated that the convective adjustment parameters in the Betts-Miller scheme affect the grid-scale precipitation as well as the convective precipitation. Also, precipitation was found to be more sensitive to changes in the saturation pressure departure than in the adjustment time

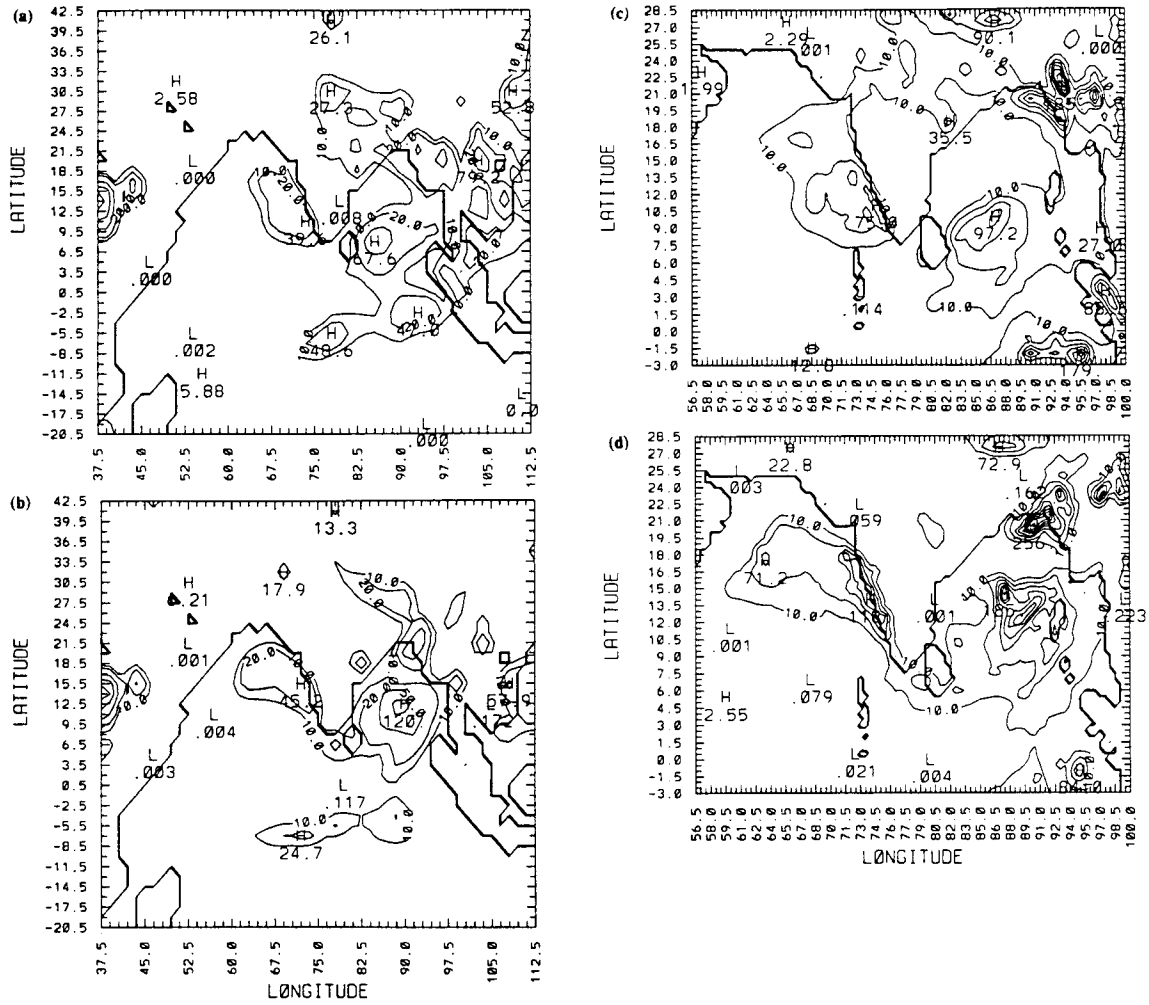

Fig. 10. Predicted rainfall for the CGM domain for a period of 24 hours ending at 12 UTC (a) 13 July and (b) 14 July, 1988 in the BMS for the CASE-6. Contour intervals are 10, 20, 50, 80 mm d^{-1}. Predicted rainfall for the FGM domain for a period of 24 hours ending at 12 UTC (a) 13 July and (b) 14 July, 1988 in the BMS for the CASE-6. Contour intervals are 10, 25, 50, 75, 100, 150 mm d^{-1}.

scale.

To evaluate the model prediction of rainfall with the Betts-Miller scheme, results from CASE-6 are compared with the observations and with the Kuo scheme. Figure 10a and 10b show the total rainfall predicted in the CGM for the first day and second day, respectively. For the first day and the second day of simulation predicted rainfall is about 39 and 45 mm d^{-1} near the Western Ghats with maxima occurring just offshore of the west coast of India. In the control experiment (CASE-1) model did not predict rainfall along the west coast for the entire period of simulation. Also, predicted rainfall over land is higher than that in the control experiment. Predicted rainfall in the CASE-6 with the Betts-Miller scheme is comparable to that with the Kuo scheme (Figs. 5a and 6a) for both the days of simulation. There exist some differences in the predicted rainfall rates over oceanic regions in the KUO and the BMS. Due to the lack of observational data, rainfall predictions over surrounding oceans could not be verified. Figure 10c and 10d show the total rainfall predicted in the FGM for the first day and second day, respectively for CASE-6. As expected, predicted rainfall rates are higher than those in the CGM and much higher than those in CASE-1. Comparing with the rainfall rates predicted using the Kuo scheme (Figs. 5c and 6c), it can be noticed that in CASE-6 predicted rainfall over land (northwest regions of India) is far lower than those obtained with the Kuo scheme.Though predicted rainfall rates along the west coast of India with the Kuo and the Betts-Miller scheme are comparable with the observations, the Betts-Miller scheme still fails to predict rainfall

Table 2. Comparison of observed and predicted rainfall maxima associated with the Western Ghats.

Description	24 Hours ending 12 UTC 13 July		24 Hours ending 12 UTC 14 July	
	Rate (mm/day)		Rate (mm/day)	
	CGM	FGM	CGM	FGM
Observations	110	110	140	140
Kuo	20	73	48	144
Betts-Miller CASE-1	0	10	13	23
CASE-2	0	20	16	33
CASE-3	0	49	16	86
CASE-4	16	69	21	95
CASE-5	35	72	35	111
CASE-6	39	75	45	118

over land regions reasonably. Also, over northern and central Bay of Bengal, large rainfall rates (185 and 256 mm d^{-1}) are predicted in the CASE-6 with the Betts-Miller scheme while with the Kuo scheme these rates are negligible (10 to 30 mm d^{-1}).

It can be seen that with the Kuo scheme predicted rainfall rates are higher than those with the Betts-Miller scheme while the evaporation rates are higher with the Betts-Miller scheme. Temporal variation of forecast errors (not shown) for the zonally averaged specific humidity indicated that model atmosphere is relatively humid with the Betts-Miller scheme. Also, forecast errors in the circulation patterns near the Western Ghats region are marginally different with both the schemes.

It can be seen that the upper limit for the τ can be as high as about 2 hours while the lower limit depends on the model horizontal resolution. To determine the lower limit of τ for the fine-grid mesh domain, another experiment with τ as 500 s was performed while keeping the τ value for the CGM same as that in the CASE-6. It was found that model predictions are very similar to that in the CASE-6 for the FGM except that during 6th and 10th hour of simulation computed sub-grid scale rainfall was negative and is about -0.1 to -0.3 mm hr^{-1}. Since negative rainfall was not allowed in the model simulations, it has no effect on the subsequent integration of the model. This negative precipitation is a direct result of the rapid adjustment of the model toward the prescribed thermodynamic profiles and also due to insufficient time given to the large-scale forcing to moisten the model atmosphere. For these reasons, the lower limit on τ for the present study of monsoon rainfall simulations can be considered as 600 s for the FGM domain.

Table 2 gives a summary of the model predicted rainfall maxima near the Western Ghats for all of the cases in the Coarse-Grid Mesh and the Fine-Grid Mesh domains during the two days of simulation using the Kuo and the Betts-Miller cumulus parameterization schemes along with the observed rainfall rates. It can be seen that wih the Kuo scheme, predicted rainfall rates for the FGM domain are closer to the observations. With the Betts-Miller scheme, there is a gradual improvement of rainfall predictions from the CASE-1 to the CASE-6. Also, spatial distribution of rainfall showed increased aerial coverage from CASE-1 to the CASE-6. Thus, results from the CASE-6 are the best in terms of comparison to those from the Kuo scheme and the observations.

5. Summary and conclusions

A ten-layer primitive equation limited area nested grid model was used to study the performance of the Kuo and the Betts-Miller cumulus parameterization schemes and the role of the horizontal grid resolution in simulating the orographic-convective rainfall associated with the mountains along the west coast of India. Two numerical experiments were performed for 48 hours using the Kuo and the Betts-Miller cumulus parameterization schemes. The initial conditions for the model integrations were obtained from the ECMWF analysis.

As expected, fine-grid resolution (FGM) model results compare better with the observations than those of the coarse-grid resolution (CGM). With the Kuo scheme, predicted rainfall rates along the west coast of India and over other land regions are comparable to those in the observations. With the Betts-Miller scheme, model underpredicted rainfall rates by about an order of magnitude. Previous studies (Betts, 1986; Baik *et al.*, 1990b; Puri and Miller, 1990) indicate that the convective adjustment parameters used in the Betts-Miller scheme are good for simulating a tropical cyclone. To find out the relevancy of values used for these adjustment parameters for the monsoon region, five sensitivity experiments are performed by systematically changing the values.

Relaxation time scale (τ) and saturation pressure departure (S) are two key adjustment parameters in the Betts-Miller scheme. The values of τ and S are changed systematically to determine the model sensitivity to these adjustment parameters. Results indicate that a significiant decrease in the τ values leads to only a minor improvement in rainfall predictions. It was also found that for a give horizontal resolution of the model there exists a lower limit on the τ value. Decrease of τ for the CGM from 7200 to 1800 s showed negligible improvement in the rainfall predictions. So, further decrease in τ for the CGM may not result in improvement in the rainfall predictions. Also, it may not be critically important to find out the lower limit of τ for the CGM as the CGM is mainly used to capture the synoptic scale monsoon circulations and to provide lateral bound-

ary conditions to the FGM. The lower limit for τ the finer-grid model is found to be about 600 s. Further decrease in the τ value in the FGM leads to a reduction in the predicted rainfall rates. This is due to the fact that as the relaxation time scale becomes smaller, adjustment of the model atmosphere towards the prescribed thermodynamic reference profiles becomes more rapid. This rapid adjustment does not allow large scale forcing to moisten the atmosphere sufficiently.

However, predicted rainfall rates are found to be more sensitive to the changes in the saturation pressure departure parameter. A decrease of 20 hPa in the value of saturation pressure departure at the lowest level of the model (level closer to the ground) resulted in a significant improvement in the model predictions of rainfall. It is found that major improvement occurs when S is decreased from -30 to -40 hPa. Further decrease in the S value to -50 hPa leads to only slight changes in the rainfall rates. Also, spatial distribution of rainfall with $S = -50$ hPa is similar to those obtained with $S = -40$ hPa but with a slight increase (by about 7 mm d^{-1}) in the maximum near the Western Ghats. This result suggests that further decrease of S value may not result in the improvement of rainfall predictions. Also, further decrease in the S value may result in unrealistic rainfall predictions during early hours of simulation. Thus, for the monsoon conditions present during the simulation period, $S = -50$ hPa appears to give better rainfall rates comparable to observations near the Western Ghats region.

Though predicted rainfall rates with the Kuo scheme are closer to the observations near the Western Ghats region, some differences do exist between model prediction and observed rainfall rates over northwest regions of India. With the Betts-Miller scheme these differences are very large over land regions with the exception to the Western Ghats. Also, predicted rainfall rates over surrounding oceanic regions (Bay of Bengal, Indian Ocean and Arabian Sea) differ significantly with the Kuo and the Betts-Miller schemes. Performance comparison of these two schemes over the oceans could not be made due to lack of observations.

Though this is a single case study, it highlights the role of key adjustment parameters in the Betts-Miller scheme and suggests suitable values for the monsoon region. Increased model vertical resolution with better boundary layer physics, inclusion of shallow convection in both the Kuo and the Betts-Miller schemes and a diabatic initialization scheme to initialize the data among other improvements will be necessary to improve the model predictions over land regions.

Acknowledgments

The authors would like to acknowledge Dr. U.C. Mohanty, National Center for Medium Range Weather Forecast, for his help in providing data and rainfall charts. This work was supported by the Naval Research Laboratory, Washington, D.C. Computer resources were provided by the North Carolina Supercomputing Program, Research Triangle Park, NC.

References

Anthes, R.A., 1977: A cumulus parameterization scheme utilizing a one-dimensional cloud model. *Mon. Wea. Rev.*, **105**, 207–286.

Arakawa, A. and W.H. Schubert, 1974: Interaction of a cumulus cloud ensemble with the large-scale environment, Part I. *J. Atmos. Sci.*, **31**, 674–701.

Baik, J.-J., M. DeMaria and S. Raman, 1990a: Tropical cyclone simulations with the Betts convective adjustment scheme. Part I: Model description and control simulation. *Mon. Wea. Rev.*, **118**, 513–528.

Baik, J.-J., M. DeMaria and S. Raman, 1990b: Tropical cyclone simulations with the Betts convective adjustment scheme. Part II: Sensitivity experiments. *Mon. Wea. Rev.*, **118**, 529–541.

Betts, A.K., 1982: Saturation point analysis of moist convective overturning. *J. Atmos. Sci.*, **39**, 1484–1505.

Betts, A.K., 1986: A new convective adjustment scheme. Part I: Observational and theoretical basis. *Quart. J. Roy. Meteor. Soc.*, **112**, 677–691.

Businger, J.A., J.C. Wyngaard, Y. Izumi and E.F. Bradley, 1971: Flux-profile relationship in the atmospheric surface layer. *J. Atmos. Sci.*, **28**, 181–189.

Das, S., U.C. Mohanty and O.P. Sharma, 1988: Study of Kuo-type cumulus parameterizations during different epochs of the Asian summer monsoon. *Mon. Wea. Rev.*, **116**, 715–729.

Davies, H.C., 1976: A lateral boundary formulation for multi-level prediction models. *Quart. J. Roy. Meteor. Soc.*, **102**, 405–418.

Devies, H.C., 1983: Limitations of some common lateral boundary schemes used in regional NWP models. *Mon. Wea. Rev.*, **11**, 1002–1012.

Geleyn, J.-F., 1985: On a simple, parameter-free partition between moistening and precipitation in the Kuo scheme. *Mon. Wea. Rev.*, **113**, 405–407.

Gronas, S., A. Foss and M. Lystad, 1987: Numerical simulations of polar lows in the Norwegian Sea. *Tellus*, **39A**, 334–353.

Grossman, R.L. and D.R. Durran, 1984: Interaction of low-level flow with the western Ghat Mountains and offshore convection in the summer monsoon. *Mon. Wea. Rev.*, **112**, 652–672.

Junker, N.W. and J.E. Hoke, 1990: An examination of nested grid model precipitation forecasts in the presence of moderate-to-strong low-level southerly inflow. *Wea. Forecasting*, **5**, 333–344.

Kuo, H.L., 1965: On the intensification of tropical cyclones through latent heat release by cumulus convection. *J. Atmos. Sci.*, **22**, 40–63.

Kuo, H.L., 1974: Further studies of the parameterization of the influence of cumulus convection of large-scale flow. *J. Atmos. Sci.*, **31**, 1232–1240.

LeMone, M.A., 1989: The influence of vertical wind shear on the diameter of cumulus clouds in CCOPE. *Mon. Wea. Rev.*, **117**, 1480–1491.

Madala, R.V., S.W. Chang, U.C. Mohanty, S.C. Madan, R.K. Raliwal, V.B. Sarin, T. Holt and S. Raman, 1987: Description of the Naval Research Laboratory limited area dynamical weather prediction model. NRL Memo. Rep., No. 5992, Naval Research Laboratory, Washington, D.C., 131 pp.

Manabe, S., J. Smagorinski and R.F. Stirickler, 1965: Simulated climatology of general circulation model with a hydrological cycle. *Mon. Wea. Rev.*, **93**, 769–798.

Ogura, Y. and M. Yoshizaki, 1988: Numerical study of orographic-convective precipitation over the eastern Arabian Sea and the Ghat mountains during the summer monsoon. *J. Atmos. Sci.*, **45**, 2097–2122.

Puri, K. and M.J. Miller, 1990: Sensitivity of ECMWF analyses-forecasts of tropical cyclones to cumulus parameterization. *Mon. Wea. Rev.*, **118**, 1709–1741.

Smith, R.B. and Y.-L. Lin, 1983: Orographic rain on the western Ghat. *Proc. First Sino-American Workshop on Mountain Meteorology*, E.R. Reiter, Z. Baozhen and Q. Younghu, Eds., 71–94.

Vukicevic, T. and R.M. Errico, 1990: The influence of artificial and physical factors upon predictability estivates rsing a complex limited-area model. *Mon. Wea. Rev.*, **118**, 1460–1482.

Kuo と Betts-Miller の積雲対流パラメタリゼーション・スキームを用いた地形性の対流性降雨の数値シミュレーション

Kiran Alapaty・Rangarao V. Madala[1]・Sethu Raman

(米国ノースカロライナ州立大学海洋地球大気科学部)

2つの異なる積雲対流パラメタリゼーションである Kuo と Betts-Miller のスキームを用いて、西ゴーツ山脈に関連した地形性の対流性降雨を、モンスーンの雨が並もしくは多かった2日間についてシミュレートする。数値シミュレーションには、プリミティブ方程式による10層狭領域ネスティッド格子モデルを用いる。Kuo スキームで予想された西ゴーツ山脈付近の降雨は観測とよく一致しているが、Betts-Miller スキームではこの領域の雨は予想されなかった。

Betts-Miller スキームで用いられた調節パラメータの不確定性を明らかにするために、5つの感度実験を行った。それぞれの実験では、緩和時間と飽和気圧差という2つの調節パラメータに異なる値を与える。感度実験の結果は、緩和時間の与え方がモデルの水平解像度に依存することを示しており、水平解像度が増加するにつれて小さくする必要がある。また雨の予想は、緩和時間の値より飽和気圧差の値に敏感である。飽和気圧差を少し変えることによって基準となる熱力学的なプロファイルが変わり、雨の予想が改善される。モンスーン地域における緩和時間と飽和気圧差の値には、それより小さくしても降水量の予想が改善されないような下限が存在することもわかった。

[1]現在所属：米国海軍研究所